



Activity-dependent modulation of inhibitory synaptic kinetics in the cochlear nucleus

Jana Nerlich¹, Christian Keine¹, Rudolf Rübsamen¹, R. Michael Burger² and Ivan Milenkovic^{3*}

¹ Department of Neurobiology, Faculty of Biosciences, Pharmacy and Psychology, University of Leipzig, Leipzig, Germany

² Department of Biological Sciences, Lehigh University, Bethlehem, PA, USA

³ Department of Physiology, Faculty of Medicine, Carl Ludwig Institute for Physiology, University of Leipzig, Leipzig, Germany

Edited by:

Conny Kopp-Scheinflug,
Ludwig-Maximilians-University
Munich, Germany

Reviewed by:

Nace L. Golding, The University of
Texas, USA

Yong Lu, Northeast Ohio Medical
University, USA

Michael Hideki Myoga,
Ludwig-Maximilians-Universität
München, Germany

*Correspondence:

Ivan Milenkovic, Department of
Physiology, Faculty of Medicine,
Carl Ludwig Institute for Physiology,
University of Leipzig, Liebigstrasse
27, Leipzig, 04103, Germany
e-mail: Ivan.Milenkovic@
medizin.uni-leipzig.de

Spherical bushy cells (SBCs) in the anteroventral cochlear nucleus respond to acoustic stimulation with discharges that precisely encode the phase of low-frequency sound. The accuracy of spiking is crucial for sound localization and speech perception. Compared to the auditory nerve input, temporal precision of SBC spiking is improved through the engagement of acoustically evoked inhibition. Recently, the inhibition was shown to be less precise than previously understood. It shifts from predominantly glycinergic to synergistic GABA/glycine transmission in an activity-dependent manner. Concurrently, the inhibition attains a tonic character through temporal summation. The present study provides a comprehensive understanding of the mechanisms underlying this slow inhibitory input. We performed whole-cell voltage clamp recordings on SBCs from juvenile Mongolian gerbils and recorded evoked inhibitory postsynaptic currents (IPSCs) at physiological rates. The data reveal activity-dependent IPSC kinetics, i.e., the decay is slowed with increased input rates or recruitment. Lowering the release probability yielded faster decay kinetics of the single- and short train-IPSCs at 100 Hz, suggesting that transmitter quantity plays an important role in controlling the decay. Slow transmitter clearance from the synaptic cleft caused prolonged receptor binding and, in the case of glycine, spillover to nearby synapses. The GABAergic component prolonged the decay by contributing to the asynchronous vesicle release depending on the input rate. Hence, the different factors controlling the amount of transmitters in the synapse jointly slow the inhibition during physiologically relevant activity. Taken together, the slow time course is predominantly determined by the receptor kinetics and transmitter clearance during short stimuli, whereas long duration or high frequency stimulation additionally engage asynchronous release to prolong IPSCs.

Keywords: inhibition, activity-dependent decay, re-uptake, intersynaptic pooling, asynchronous release, spherical bushy cell, cochlear nucleus

INTRODUCTION

Synaptic inhibition is mainly mediated by glycine and GABA_A receptors (GlyR and GABA_AR, respectively) which tightly regulate neuronal and network activities. While the GlyR-generated inhibitory postsynaptic current (IPSC) is generally endowed with fast decay kinetics (Takahashi et al., 1992; Awatramani et al., 2004), GABA provides slow and in some cases tonic inhibition (Farrant and Nusser, 2005; Capogna and Pearce, 2011; Tang et al., 2011). Notably, there are presynaptic terminals in the sensory systems (Wentzel et al., 1993; Protti et al., 1997; Apostolides and Trussell, 2014), cerebellum (Dumoulin et al., 2001; Rousseau et al., 2012; Husson et al., 2014) and in the spinal cord (Jonas et al., 1998; O'Brien and Berger, 1999; Keller et al., 2001; Seddik et al., 2007) that release both transmitters beyond the early postnatal development. This allows for an additional variability, through activity-dependent use of transmitters (Nerlich et al., 2014), differential distribution of respective receptors at the same cell (Chéry and de Koninck, 1999), at different cells (Dugué

et al., 2005; Kuo et al., 2009), or shaping the IPSC decay through action of both glycine and GABA on GlyR (Lu et al., 2008).

The postsynaptic responses in neurons expressing both GlyR and GABA_AR usually represent a mixture of respective fast and slow synaptic currents (Russier et al., 2002; Awatramani et al., 2005; González-Forero and Alvarez, 2005; Coleman et al., 2011; Apostolides and Trussell, 2013). The relative contribution of both physiologically important components can change according to the activity pattern (Fischl et al., 2014). Such activity-dependent inhibitory control, mediated by dual glycine-GABA signaling, has been recently shown for the spherical bushy cells (SBCs) in the central auditory system (Nerlich et al., 2014). SBCs receive acoustically evoked excitatory input from auditory nerve fibers through large calyceal terminals, the endbulbs of Held (Ryugo and Sento, 1991; Isaacson and Walmsley, 1996; Nicol and Walmsley, 2002), and non-primary inhibition from neurons within the cochlear nucleus (Wickesberg and Oertel,

1990; Saint Marie et al., 1991; Campagnola and Manis, 2014). The amplitude of IPSCs is dominated by GlyRs, while the initially small GABAergic component successively enhances the inhibitory strength and shapes its duration at physiologically relevant rates (Nerlich et al., 2014). Unlike other central auditory synapses that utilize phasic inhibition even at high rates (Awatramani et al., 2004; Kramer et al., 2014), IPSCs in SBCs summate due to slow kinetics (Xie and Manis, 2013, 2014; Nerlich et al., 2014), thereby providing a functionally tonic inhibition, similar to inhibition acting on the granule cells in the dorsal cochlear nucleus (DCN) and nucleus magnocellularis neurons in the cochlear nucleus of the chick (Lu and Trussell, 2000; Monsivais et al., 2000; Balakrishnan et al., 2009). To date, the synaptic mechanisms that determine the slow kinetics of the mixed glycine-GABA transmission in SBCs remained elusive.

We examined the mechanisms underlying the slow activity-dependent IPSC kinetics in SBCs by performing whole-cell recordings in acute slice preparations of juvenile Mongolian gerbils in combination with synaptic stimulation of inhibitory inputs. Our results demonstrate that the low capacity of glycine and GABA uptake allows transmitter rebinding, particularly at input rates above 100 Hz. The activity-driven transmitter spillover possibly engaged distant GlyR but not GABA_AR. Synaptic activity largely desynchronized the release of glycine and GABA, which had a significant contribution to the slow IPSC profile.

MATERIALS AND METHODS

The experimental procedures were approved by the Saxonian district Government Leipzig (T 84/12, T 67/13) and conducted according to the European Communities Council Directive (86/609/EEC).

SLICE PREPARATION

Coronal slices (180 μm) containing the rostral anteroventral cochlear nucleus (AVCN) were cut from P22-P30 gerbils of either sex. The brainstem was sliced with a vibratome in low-calcium artificial cerebrospinal fluid (ACSF) solution containing (in mM): 125 NaCl, 2.5 KCl, 0.1 CaCl_2 , 3 MgCl_2 , 1.25 NaH_2PO_4 , 25 NaHCO_3 , 25 glucose, 2 sodium pyruvate, 3 myo-inositol, 0.5 ascorbic acid, continuously bubbled with 5% CO_2 and 95% O_2 , pH 7.4. Slices were incubated in the standard recording solution (ACSF same as for slicing, except CaCl_2 and MgCl_2 were changed to 2 mM and 1 mM, respectively) for 30 min at 37°C and stored at room temperature until recording. Experiments were performed at nearly physiological temperature ($33.5 \pm 0.5^\circ\text{C}$).

ELECTROPHYSIOLOGICAL RECORDINGS

Whole-cell patch clamp recordings were performed on SBCs in the rostral pole of the AVCN. Due to their large soma size and localization in the low-frequency area of the gerbil AVCN, these neurons can be visually distinguished from globular bushy cells. Morphological verification of SBCs was done during the recording by intracellular labeling with ATTO 488 and visualization by a CCD camera (IMAGO Typ VGA; TILL Photonics). The pipettes had resistances of 3–4 $\text{M}\Omega$ when filled with (mM):

125 CsMeSO_3 , 18 TEA-Cl, 3 MgCl_2 , 10 HEPES, 0.1 EGTA, 4.5 QX-314-Cl, 5 phosphocreatine, 2 ATP disodium salt, 0.3 GTP disodium salt, and 50 μM ATTO 488 (pH 7.3 with CsOH). The resulting inward currents with larger amplitudes enabled more accurate analyses compared to the small events occurring with physiological $[\text{Cl}^-]_{\text{pip}}$. Consistent with slow inhibitory kinetics in the present study, the synaptically evoked hyperpolarizations acquired with gramicidin perforated patch recordings also exhibited slow activity-dependent synaptic decays (gramicidin perforated patch: t_{wd} single: 18.5 ± 4.0 ms, 100 Hz 10th IPSC: 42.6 ± 4.1 ms, $n = 6$, see Nerlich et al., 2014). IPSCs were evoked by electrical stimulation of afferent fibers through a bipolar theta glass electrode (Science Products, tip \varnothing 5 μm) filled with bath solution and placed at distances of 30–60 μm from the cell. Pulse stimuli (100 μs , 15–90 V) were generated by a stimulator (Master 8) and delivered via a stimulus isolation unit (AMPI Iso-flex) to evoke either single events or train-responses at different frequencies. Voltage clamp measurements were done from $V_{\text{hold}} = -71$ mV, (Nerlich et al., 2014), except in cases where the amplitudes of the small asynchronous events were increased for precise event detection by holding the cell at -81 mV (Figure 5). To isolate glycine- and GABA_A receptor mediated signals, a pharmacological inhibition of glutamate (50 μM AP-5, 10 μM NBQX) and GABA_B receptors (3 μM CGP 55845) was performed in all experiments. Offline correction of voltages was done for junction potentials of 11 mV. For some experiments, the extracellular calcium concentration in the ACSF was reduced to 1.2 mM in order to decrease the release probability. In such cases, the magnesium concentration was simultaneously increased to 1.8 mM to maintain the concentration of divalent cations.

DATA ACQUISITION AND ANALYSIS

The recordings were acquired using a Multiclamp 700B amplifier (Molecular Devices). The mean capacitance of the cells was 23.15 ± 4.34 pF (mean \pm SD, $n = 52$). The average series resistance was 11.25 ± 1.56 $\text{M}\Omega$ ($n = 52$), which was compensated by 50% to a remaining R_s of 3–7 $\text{M}\Omega$. During experiments the series resistance changed on average by 2.6% ($n = 52$). Cells with series resistance changes $>10\%$ were excluded from analysis. There was no correlation between the IPSC amplitudes and decay time constants ($r_s = 0.17$, $p = 0.22$, $n = 53$). Together with the previously reported lack of correlation between the IPSC amplitudes and rise times ($r_s = 0.04$, $p = 0.78$, $n = 43$, Nerlich et al., 2014), these data rule out the possible contribution of series resistance error to decay time constant measurements. Recorded signals were digitized at 50 kHz and filtered with a 6 kHz Bessel low-pass filter. Data were examined with pClamp 10 software (Molecular Devices) followed by analyses using custom-written Matlab routines (version 8.3, Mathworks, Natick). Mean amplitudes, 10–90% rise times and decay time constants of IPSCs were analyzed from averaged traces (>5 repetitions). For detection of asynchronous release events, the current traces were band-pass filtered between 50 and 1500 Hz using a zero-phase forward and reverse digital IIR filter to remove the decay component (see Figure 5A). Statistical analysis by means of z -test revealed events with current amplitudes exceeding 1.96 times ($p < 0.05$)

the standard deviation of the baseline. To avoid multiple triggers of the same event, all triggers occurring within 5 ms after the preceding event were excluded from the analysis. The results were visually controlled to ensure the correct detection of spontaneous events. The events occurring prior to electrical stimulation (spontaneous IPSCs) were quantified and compared to events emerging after the end of synaptic stimulation of inhibitory inputs. Asynchronous events were clearly visible during the decay phase of the last evoked IPSC. Events detected by the software during the first 20 ms of the current decay were not included in the analysis to avoid false positive results. Data from 3 repetitions for each condition were pooled and presented for each cell.

IPSC decay phase was fitted with mono- or bi-exponential functions based on an increase in adjusted R^2 values. The weighted τ decay was calculated as $\tau_{wd} = (A_{fast} \times \tau_{fast} + A_{slow} \times \tau_{slow}) / (A_{fast} + A_{slow})$, where A_{fast} and A_{slow} are amplitudes at $t = 0$ and τ_{fast} and τ_{slow} are the fast and slow time constants, respectively. In cases of mono-exponential fits, one exponential component was set to 0.

STATISTICS

Data sets were compared with the appropriate t -test or analysis of variance (ANOVA). The p -values of multiple comparisons were adjusted by the Dunn-Šidak procedure. Within-subject comparisons were performed by repeated-measures (RM) ANOVA after testing for sphericity using Mauchly test, and Greenhouse-Geissner correction applied as appropriate. ANOVA was used to test for effects of drugs and possible interactions of input frequency and drug superfusion. The changes in asynchronous release evoked by different input frequencies were tested for significance by a z -test, $z = (A - BL) / SD_{BL}$, with A being the average number of events/bin 20–60 ms after stimulation, BL the mean of the baseline (1 s prior to stimulation = spontaneous IPSC level) and SD_{BL} the standard deviation of the baseline. All data are reported as mean \pm SEM, unless otherwise stated.

RESULTS

IPSC DECAY RATE IS ACTIVITY-DEPENDENT

SBCs exhibit slow inhibitory synaptic decays (Figure 1A) mediated by GlyR and GABA_AR (gerbil: spontaneous IPSCs: $\tau_{wd} = 16.7 \pm 1.2$ ms, synaptically evoked IPSCs $\tau_{wd} = 23.7 \pm 5.3$ ms, Nerlich et al., 2014; mouse: spontaneous IPSCs: $\tau_{wd} = 8.75 \pm 0.6$ ms, synaptically evoked IPSCs $\tau_{wd} = 11.1 \pm 0.8$ ms, Xie and Manis, 2013). Both the glycinergic and the GABAergic components were observed in all pharmacology experiments acquiring IPSCs with suprathreshold stimulation to evoke reliable responses (see also Nerlich et al., 2014). Notably, the pharmacologically isolated glycinergic and GABAergic single events were previously shown to have similar kinetics (Nerlich et al., 2014), thus arguing against the hypothesis that in SBCs the fast decay component can be accounted to glycine and the slow component to GABA. In the present study we investigated the underlying mechanism determining such inhibitory current kinetics. The decay phase of synaptically evoked single IPSCs was best fit with a bi-exponential function with a fast decay time constant $\tau_{fast} = 8.7 \pm 2.1$ ms, a slow decay time constant $\tau_{slow} = 38.9 \pm 7.2$ ms and their respective

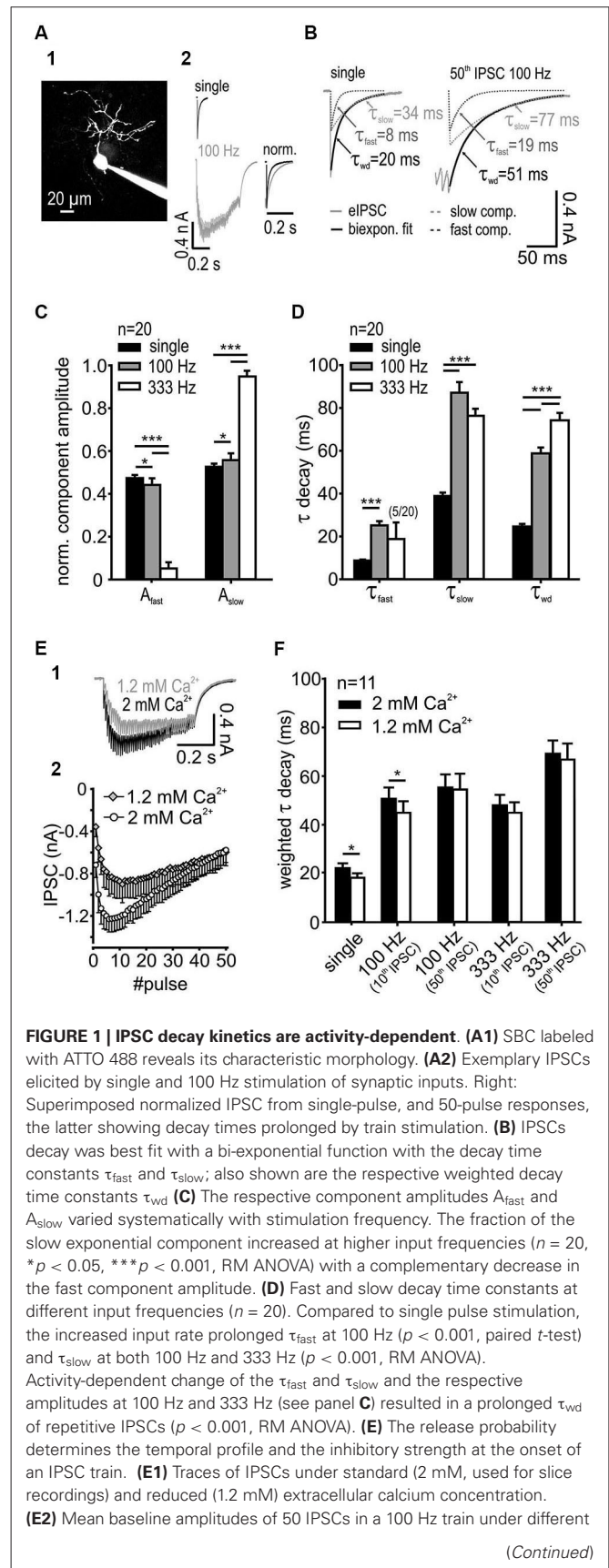


FIGURE 1 | Continued

extracellular calcium concentrations ($n = 6$). **(F)** For single IPSCs and the 10th IPSC at 100 Hz the weighted decay time constant was shorter under 1.2 mM extracellular calcium. $[Ca^{2+}]_o$ had no influence on τ_{wd} at longer trains of IPSCs (50 pulses) or at higher input frequency (333 Hz) ($n = 11$, single and 100 Hz 10th $p < 0.05$, 100 Hz 50th, 333 Hz 10th and 50th, $p > 0.27$, RM ANOVA).

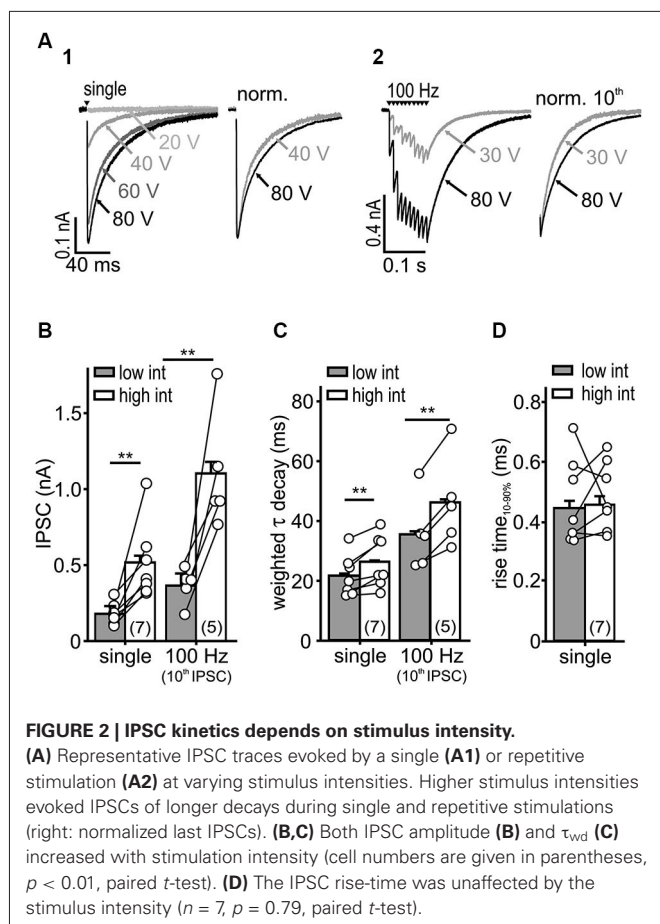
relative amplitudes $A_{fast} = 0.47 \pm 0.06$ and $A_{slow} = 0.53 \pm 0.06$. The resulting average weighted decay time constant for 20 SBCs was $\tau_{wd} = 24.7 \pm 5.4$ ms (mean \pm SD). The synaptic current decays were progressively slower after repetitive stimulation of inputs and with increasing input frequencies (**Figures 1B,D**). Also, the relative amplitude of the slow exponential component increased with input rates (**Figure 1C**; A_{slow} single = 0.53 ± 0.06 , 100 Hz = 0.56 ± 0.03 ; 333 Hz = 0.95 ± 0.03 , single vs. 100 Hz $p < 0.05$; 100 Hz vs. 333 Hz $p < 0.001$, $n = 20$, RM ANOVA). Complementary decrease in amplitude of the fast component occurred over the same range of stimuli (A_{fast} single = 0.47 ± 0.06 , 100 Hz = 0.44 ± 0.03 , 333 Hz = 0.05 ± 0.03). The slow decay time constant was prolonged substantially at 100 Hz and 333 Hz (**Figure 1D**; τ_{slow} single = 38.9 ± 1.6 ms, 100 Hz = 87.1 ± 5.0 ms, 333 Hz = 76.3 ± 3.3 ms, $n = 20$, $p < 0.001$ for single vs. 100 Hz and 333 Hz, RM ANOVA). At 333 Hz, the decay phase was best fit with a mono-exponential function excluding the fast exponential component in 75% of recorded SBCs (in these cells A_{fast} was set to 0). Due to the rare occurrence of τ_{fast} at 333 Hz (only in 5 out of 20 cells), this parameter was statistically compared only for the single and 100 Hz stimulation. The τ_{fast} was prolonged at 100 Hz compared to single pulse stimulation (τ_{fast} single = 7.1 ± 0.6 , 100 Hz = 21.4 ± 3.0 , $n = 20$, single vs. 100 Hz $p < 0.001$, paired t -test). Activity-dependent change of τ_{fast} , τ_{slow} and the respective amplitudes resulted in a prolongation of τ_{wd} with increasing input frequency (**Figure 1D**; τ_{wd} single = 24.7 ± 1.2 ms, 100 Hz = 58.8 ± 2.8 ms, 333 Hz = 74.2 ± 3.5 ms, $n = 20$, $p < 0.001$ for all comparisons, RM ANOVA). However, the longer decays were not associated with larger IPSC amplitudes (τ_{wd} single = 22.8 ± 0.8 ms, 50th 100 Hz = 61.8 ± 2.5 ms, $n = 25$, $p < 0.001$, paired t -test; IPSC amplitude single = 0.56 ± 0.5 nA, 50th 100 Hz = 0.55 ± 0.04 nA, $n = 25$, $p = 0.81$, paired t -test), thus suggesting that activity-dependent synaptic mechanisms, rather than series resistance errors cause the decay time prolongation. Together, these data indicate that the increase in input rates increases the transmitter quantity in the cleft which particularly prolongs the τ_{slow} through transmitter rebinding.

Studies at the calyx of Held-MNTB principal neuron synapse revealed that *in vivo* release probability may be approximated in slice recordings by using 1.2 mM Ca^{2+} in the extracellular solution (Borst, 2010). The dependence of the IPSC decay times on the release probability was shown at other auditory synapses (Balakrishnan et al., 2009; Tang and Lu, 2012). Although the *in vivo* release probability for the endbulb of Held-SBC synapse remains to be elucidated, we still addressed the question, whether the slow decay of inhibitory currents measured in SBCs is due to an increased release probability in the slice recordings. For

this, the weighted decay time constant was measured from the last event within trains consisting of different numbers of pulses and the results were compared for 1.2 mM and 2 mM external calcium concentration (**Figure 1F**). Single IPSCs and short trains (10 pulses at 100 Hz) revealed faster decay time constants under the lower release probability condition. However, with increasing stimulus number and frequency, the weighted decay time constant of the last pulse in the train was similar between the two calcium conditions, (**Figure 1F**; main effect calcium $p = 0.04$, 1.2 vs. 2 mM: single, 100 Hz 10th IPSC $p < 0.05$, 100 Hz 50th IPSC $p = 0.72$, 333 Hz 10th $p = 0.27$ and 50th IPSC $p = 0.33$, $n = 11$, RM ANOVA). The slower IPSC at the higher release probability could either be due to transmitter pooling or to multivesicular release. The latter mechanism could explain the data for the single and short IPSC trains. The reduction of extracellular calcium to 1.2 mM decreased the IPSCs amplitudes, especially at the onset of a 100 Hz train (50 pulses) (**Figure 1E**). However, at the end of the train the baseline IPSC amplitudes were similar to those measured under 2 mM $[Ca^{2+}]_o$ (IPSC amplitudes 2 mM vs. 1.2 mM: onset = 1st IPSC, $p < 0.001$; maximum = mean 6–8th IPSC vs. mean 10–12th IPSC, $p < 0.01$; end = mean 48–50th IPSC, $p = 0.88$, $n = 6$, RM ANOVA). Thus, the release probability is unlikely to play a role for longer trains of stimuli or high frequency stimulation pointing to transmitter pooling as a mechanism contributing to slow decays.

RECRUITMENT OF FIBERS SLOWS THE IPSC DECAY

Recruitment of nearby inputs can lead to spillover of transmitter to remote synaptic or extrasynaptic sites, and thereby to intersynaptic pooling. Thus, it is conceivable that the slow IPSC decay in SBCs is caused by ongoing rebinding of transmitter and activation of extrasynaptic receptors, as shown earlier (Balakrishnan et al., 2009; Tang and Lu, 2012). To determine whether synaptic recruitment influences the kinetics of inhibition in SBCs, IPSCs were evoked with increasing stimulus intensities (**Figure 2A**). The low intensity was set slightly above the threshold with IPSC amplitudes reaching $38.5 \pm 16\%$ (mean \pm SD, $n = 7$) of the maximal amplitude evoked by high stimulation intensity. With an increase in stimulus intensity, the amplitude of a single evoked IPSC and the last IPSC in a 100 Hz train increased threefold (**Figure 2B**; low vs. high intensity: single, $n = 7$, $p < 0.01$; 100 Hz 10th IPSC, $n = 5$, $p < 0.01$, paired t -test). Furthermore, the weighted decay time constants of single and repetitive IPSCs were prolonged at high stimulus intensities (**Figure 2C**; τ_{wd} single: low = 21.6 ± 0.6 ms, high = 26.3 ± 0.6 ms, $n = 7$, $p < 0.01$, 100 Hz 10th IPSC: low = 35.4 ± 0.8 ms, high = 46.0 ± 0.8 ms, $n = 5$, $p < 0.01$, paired t -tests). On the other hand, the rise time of single IPSCs was not dependent on stimulus intensity, suggesting the recruitment of nearby synaptic inputs (**Figure 2D**; low = 0.44 ± 0.03 ms, high = 0.46 ± 0.03 ms, $n = 7$, $p = 0.79$, paired t -test). As we neither observed a build-up, nor a run-down of IPSC amplitudes during repetitions at a given stimulus intensity, it is unlikely that the number of activated inputs changed. Therefore, these data suggest that the transmitter quantity substantially contributes to slow inhibitory kinetics.



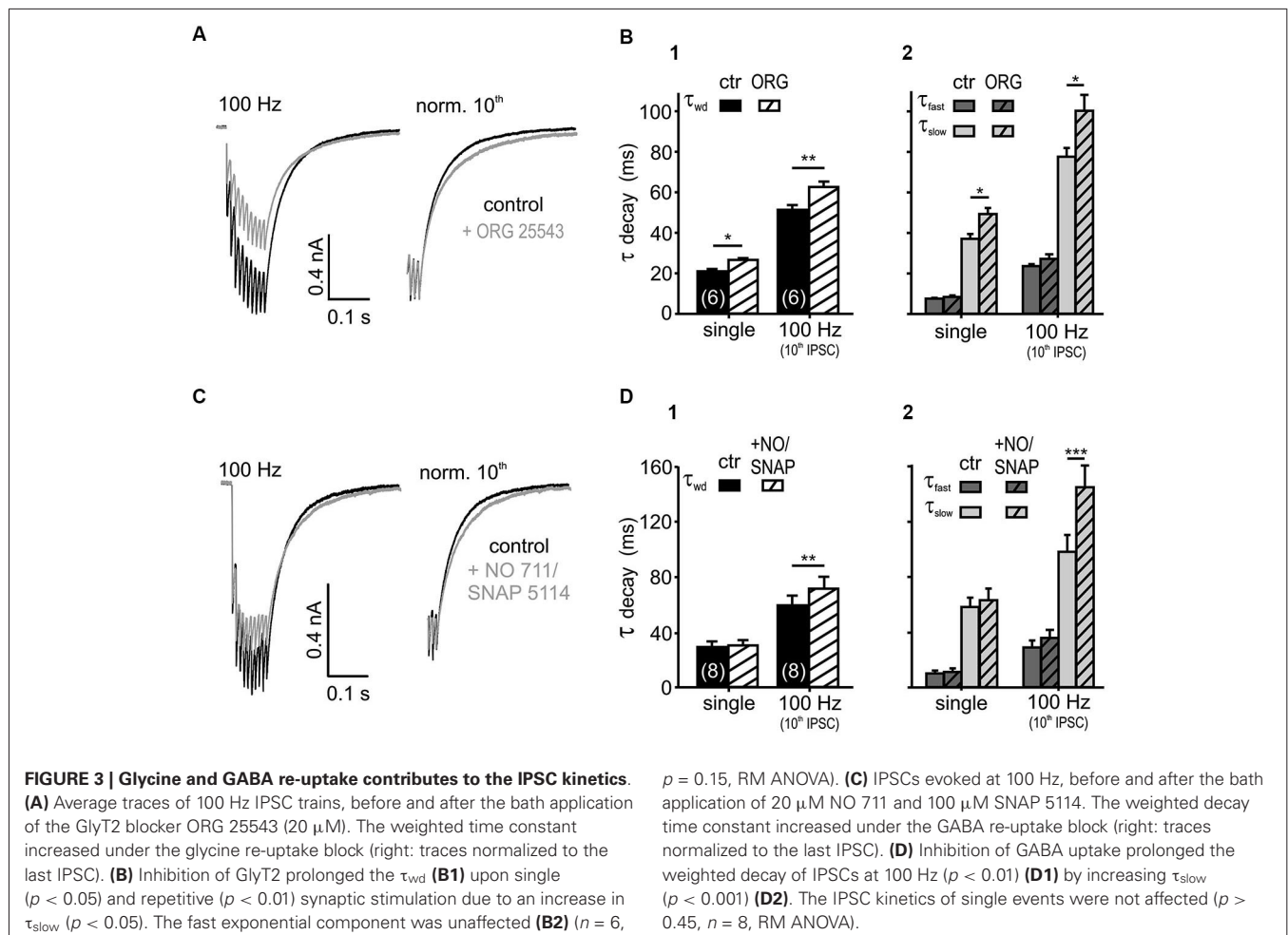
TRANSMITTER UPTAKE CONTRIBUTES TO THE IPSC KINETICS

If transmitter spillover and its clearance from the synaptic cleft shape the IPSC decay in an activity-dependent manner, the postsynaptic currents should be sensitive to a blockade of re-uptake transporters (Otis et al., 1996; Balakrishnan et al., 2009; Tang and Lu, 2012). Bath application of the glycine transporter 2 (GlyT2) inhibitor ORG 25543 (20 μ M, Bradaia et al., 2004; Balakrishnan et al., 2009) slowed down the decay of both single and train IPSCs (**Figures 3A,B**; $n = 6$, RM ANOVA). The fast decay time constant, the respective amplitudes of the exponential components and the IPSC rise time were not affected by the glycine re-uptake block ($n = 6$, control vs. +ORG, τ_{fast} : $p = 0.15$; A_{slow} and A_{fast} : $p = 0.37$, RM ANOVA, rise time: $p = 0.99$, paired t -test). Therefore, it can be concluded that the τ_{wd} prolongation (**Figure 3B**) is caused by the significantly longer τ_{slow} (**Figure 3B**). Given the similar IPSC decays of the isolated glycinergic and GABAergic single events (Nerlich et al., 2014), the τ_{fast} probably describes the intrinsic kinetics of receptor activation and de-activation, whereas the transmitter clearance, relief from saturation and delayed release determine τ_{slow} .

In addition to the sensitivity to glycine re-uptake, the IPSC decay phase was also shaped by GABA clearance. Simultaneous inhibition of the respective neuronal- and glial-GABA

transporters with 20 μ M NO 711 (Szabadics et al., 2007; Tang and Lu, 2012) and 100 μ M SNAP 5114 (Keros and Hablitz, 2005; Song et al., 2013) extended the weighted decay time constant of the last IPSC in 100 Hz trains. Again, the prolongation of τ_{slow} during re-uptake blockade underlie the slowing of train IPSCs (**Figures 3C,D**; $n = 8$, control vs. +NO/SNAP, τ_{slow} : $p < 0.001$, τ_{wd} : $p < 0.01$, RM ANOVA). Notably, the GABA uptake is apparently only contributing to the decay during ongoing activity, as single evoked IPSC decays were not affected ($p > 0.45$) (**Figure 3D**). Similar to the effects seen after blockade of glycine re-uptake, GABA re-uptake inhibition did not change the fast decay time constants, the respective amplitudes of the exponential components and the IPSC rise times ($n = 8$, control vs. +NO/SNAP, τ_{fast} : $p = 0.11$, A_{slow} and A_{fast} : $p = 0.43$, RM ANOVA, rise time: $p = 0.40$, paired t -test). Together, these data suggest that glycine rebinding caused by transmitter pooling due to slow clearance is an important factor in shaping the inhibitory current profile. On the other hand, the GABA re-uptake only contributes at high stimulus input rates to the decay kinetics, when it presumably accumulates in the synaptic cleft.

To investigate transmitter rebinding and the possible contribution of spillover to inhibitory kinetics, we assessed the effects of low affinity GlyR and GABA_AR antagonists. The rationale to use weak competitive antagonists to probe for putative remote synapses arises from studies showing that the receptors distant to the release site are likely to encounter a lower transmitter concentration during a synaptic event (Diamond, 2001; Chen and Diamond, 2002). Hence, the low-affinity competitive antagonists are progressively more effective at receptors facing low transmitter concentrations through spillover (Overstreet and Westbrook, 2003; Szabadics et al., 2007; Balakrishnan et al., 2009; Tang and Lu, 2012). Bath application of a high concentration of SR 95531 (200 μ M), employed as a low affinity antagonist of GlyR (Wang and Slaughter, 2005; Beato, 2008; Balakrishnan et al., 2009), reduced the IPSC amplitudes considerably and accelerated the weighted decay time constant of single and repetitive IPSCs (**Figures 4A–C**; $n = 6$, RM ANOVA). Low concentrations of SR 95531 (10 and 20 μ M) specifically blocked GABA_A receptors on SBCs and reduced the IPSC amplitudes by $18 \pm 2\%$ and $16 \pm 3\%$, respectively (Nerlich et al., 2014). At the concentration of 200 μ M, a $76 \pm 5\%$ reduction of the IPSC amplitude was observed (**Figure 4D**; 200 μ M vs. 10 μ M ($n = 6$), $p < 0.001$; 200 μ M ($n = 6$) vs. 20 μ M ($n = 11$), $p < 0.001$, ANOVA). This result is consistent with an additional antagonistic action of a high SR 95531 concentration at GlyR, as opposed to specific GABA_AR blockade at concentrations of 10 and 20 μ M (Nerlich et al., 2014). To further confirm the competitive antagonistic action of SR 95531 at GlyR, the glycine concentration in the cleft was increased by co-applying the glycine re-uptake inhibitor ORG 25543. This partially reversed the long τ_{wd} confirming that the current decay is regulated by the amount of available glycine (**Figure 4D**; change of τ_{wd} : +20 μ M SR = $-8.1 \pm 2.4\%$, $n = 13$; +200 μ M SR = $-35.3 \pm 2.5\%$, $n = 6$; +200 μ M SR+ORG = $-21.2 \pm 5.5\%$, $n = 6$; 20 μ M vs. 200 μ M SR $p < 0.001$, 200 μ M SR vs. 200 μ M SR+ORG $p = 0.01$, ANOVA). As the uptake blockers reveal transmitter spillover by increasing its quantity and enabling distant



receptors to encounter a lower concentration of an agonist (Chen and Diamond, 2002; Thomas et al., 2011), our data showing a decay time prolongation under ORG 25543 are consistent with glycine spillover.

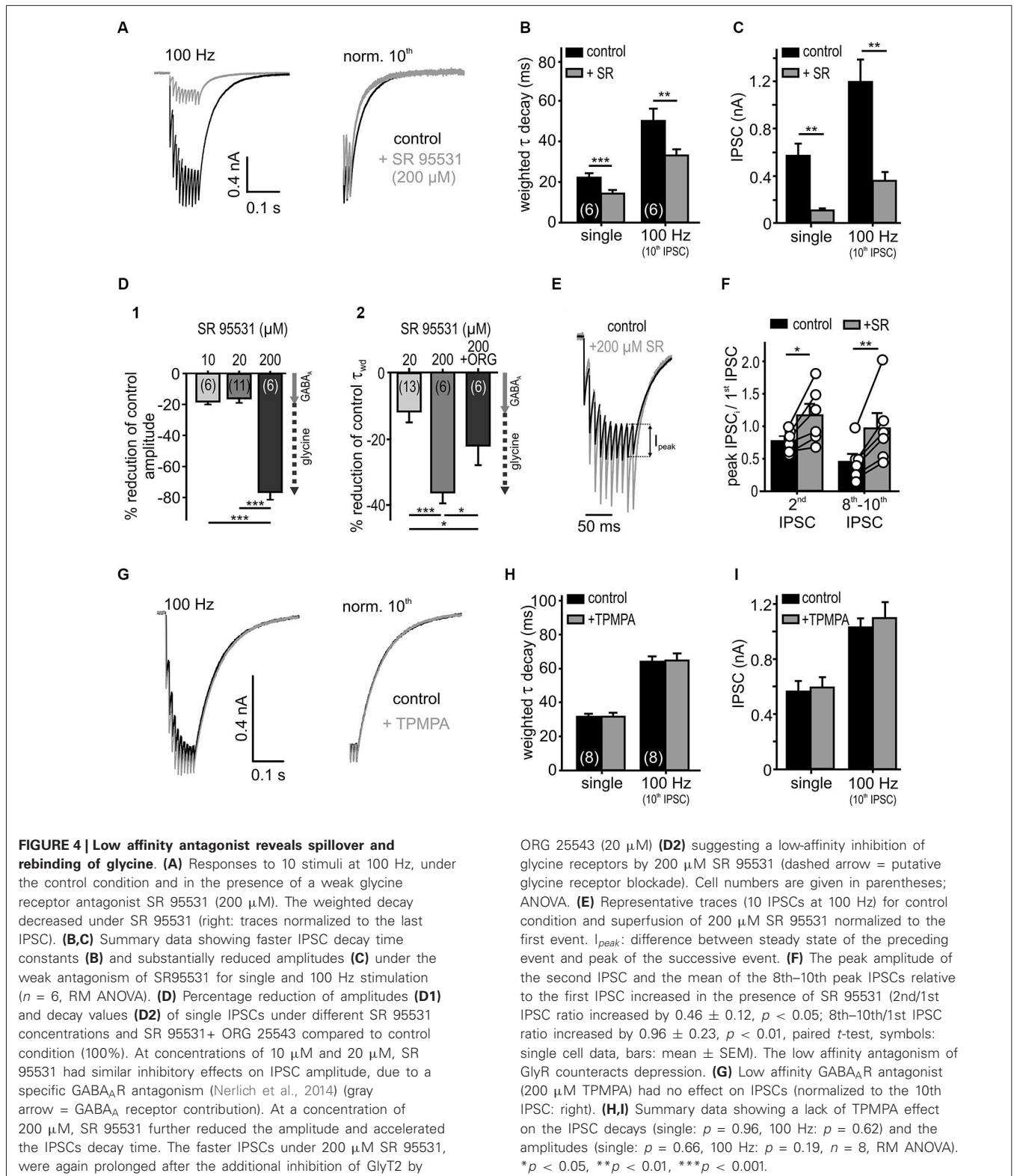
Inhibitory currents in SBCs show an activity-dependent depression of the IPSC peak amplitudes (I_{peak} , Figure 4E). Yet, under the low affinity GlyR antagonist (200 μ M SR 95531), the peak amplitudes showed a weaker depression which in some cells even changed into facilitation (Figures 4E,F). This result is consistent with a relief from receptor saturation and/or desensitization (Chanda and Xu-Friedman, 2010). Thus, the peak IPSC depression at high input rates is presumably caused by post-synaptic receptor saturation and/or desensitization, rather than presynaptic short-term plasticity.

Contrary to glycine signaling, GABA is apparently not activating nearby synapses. Even at high stimulation rates, the low affinity GABA_AR antagonist TPMPA (Szabadics et al., 2007; Tang and Lu, 2012) neither affected the IPSC decay nor the amplitudes, suggesting that the postsynaptic GABA_AR could be tightly coupled to release sites of the transmitter and, thus, encounter consistently high GABA concentration (Figures 4G–I; control vs. TPMPA τ_{wd} : single $p = 0.97$; 100 Hz 10th IPSC $p = 0.62$; IPSC

amplitude: single $p = 0.67$; 100 Hz 10th IPSC $p = 0.19$; $n = 8$, RM ANOVA). In summary, the apparently low uptake capacity of glycine and GABA transporters slows the decay of IPSCs, thereby enabling spillover of glycine. While we found no evidence for spillover of GABA, the transmitter quantity and intrinsic receptor properties probably account for the slow GABAergic transmission.

ACTIVITY-DEPENDENT ASYNCHRONOUS RELEASE

A further mechanism putatively contributing to IPSC decay time in SBCs could be an activity-induced desynchronization of vesicle release, as shown for several inhibitory synapses (Lu and Trussell, 2000; Hefft and Jonas, 2005; Tang and Lu, 2012). To test this hypothesis, high frequency stimulation (100 and 333 Hz) of inhibitory inputs to SBCs was employed to evoke small asynchronous events in the decay phase following the IPSC trains (Figure 5A). The quantity of asynchronous IPSCs increased with stimulus duration (Figures 5B,E) and frequency (Figures 5C,F). To compare the spontaneously occurring IPSCs (sIPSC, without input stimulation) and delayed IPSCs following repetitive input stimulation, the events were detected during 1 s before synaptic stimulation and 2 s after the last evoked IPSC



(see methods). The number of asynchronous events increased significantly after the 333 Hz stimulation (Figure 5E summary data for 4 cells and respective presentation of 10, 25 and 50

stimuli at 333 Hz z values > 10.1 , $p < 0.001$, z -test), compared to the rate of sIPSC before stimulation (Figure 5D; mean # of sIPSCs/20 ms bin = 0.56 ± 0.08 , $n = 4$). This result suggests

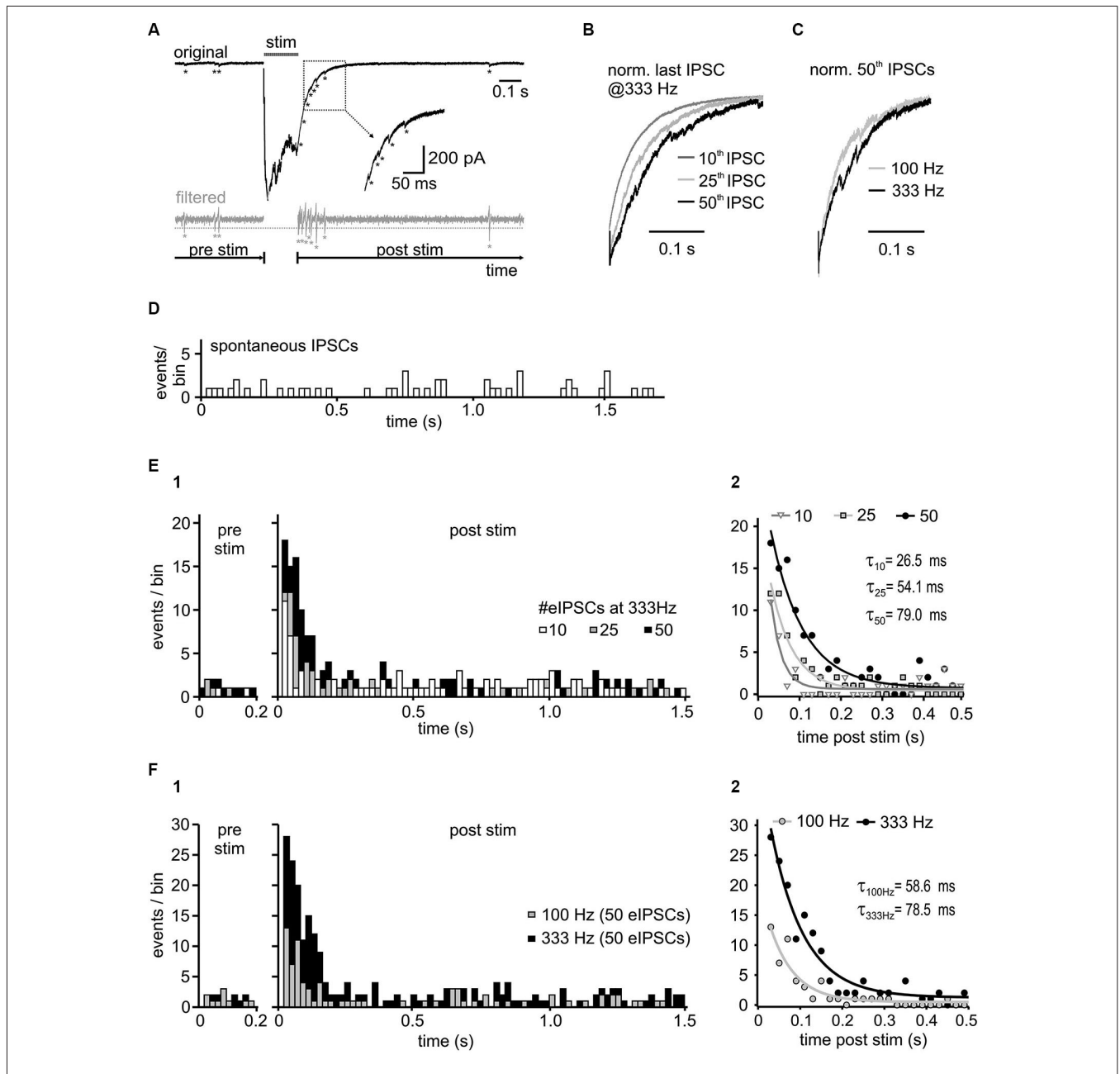


FIGURE 5 | Activity-dependence of asynchronous release. (A)

Representative trace with detected asynchronous release events, before and after 50 stimuli at 333 Hz (upper panel). For event detection the signal was bandpass filtered between 50 and 1500 Hz (bottom panel). Potential events were detected when the filtered current amplitude exceeded 1.96 times ($p < 0.05$) the standard deviation of the noise (dashed gray line). Note the increased incidence of events in the decay phase of the last IPSC. **(B)** Normalized last IPSCs elicited by different numbers of stimuli in a 333 Hz train. **(C)** Superimposed normalized last IPSCs in a 50-pulse train at 100 Hz and 333 Hz. **(D)** Histogram of spontaneous IPSCs before synaptic stimulation of inhibitory inputs ($n = 4$ cells, bin width: 20 ms). **(E1)** Histograms of asynchronous release events before (= spontaneous events, pre stim) and after the 333 Hz input stimulation (= asynchronous and spontaneous events,

post stim) with different number of stimuli ($n = 4$ cells, bin width: 20 ms, post stim $t = 0$ refers to the time of the last IPSC in the train). Following synaptic stimulation, the time course of asynchronous events relaxed back to the resting state with a mono-exponential function. The increase of asynchronous events during the decay phase depends on the presynaptic activity. **(E2)** Mono-exponential fits to the data from **(E1)**. The initial incidence of events, and the time constant (τ) depend on stimulus number (10 vs. 25 vs. 50 stimuli $p < 0.05$ for each comparison). **(F)** Input frequency determines the amount of asynchronous release. **(F1)** Summary histograms of asynchronous events from 6 cells, before and after 50-pulse stimulation at 100 Hz and 333 Hz. **(F2)** Mono-exponential fits to the data from F1. The initial incidence of events was increased and the exponential time constant prolonged with higher input frequency (100 Hz vs. 333 Hz $p < 0.05$).

the occurrence of activity induced asynchronous events in the decay phase of IPSC trains. Detailed analyses revealed the time

course of incidence of asynchronous events which was best fit with a mono-exponential function relaxing back to the resting

state. The following parameters were used to quantify the delayed release: initial amplitude (peak incidence of asynchronous events (A), an exponential time constant (τ) and a steady state value (c) (**Figure 5E**; fit comparison 10 vs. 25 vs. 50 stimuli $p < 0.001$, F -test). The peak incidence of asynchronous events after stimulation at 333 Hz increased almost 2-fold by extending the train from 10 to 50 pulses ($A_{\#eIPSC}$ 95% CI [lower, upper]: $A_{10} = 10.6$ [9.1, 12.2] events, $A_{25} = 12.9$ [11.7, 14.0] events, $A_{50} = 18.8$ [17.3, 20.3] events, 10 vs. 25 vs. 50 stimuli $p < 0.05$). The exponential time constant was also prolonged ($\tau_{\#eIPSC}$ 95% CI [lower, upper]: $\tau_{10} = 26.5$ [20.5, 37.4] ms, $\tau_{25} = 54.1$ [46.8, 64.4] ms, $\tau_{50} = 79.0$ [69.7, 91.1] ms, 10 vs. 25 vs. 50 stimuli $p < 0.05$), whereas the steady state values were similar to the mean sIPSC levels 1 s before stimulation ($c_{\#eIPSC}$ 95% CI [lower, upper]: $c_{10} = 0.63$ [0.52, 0.75] events/bin, $c_{25} = 0.43$ [0.33, 0.53] events/bin, $c_{50} = 0.73$ [0.59, 0.87] events/bin; sIPSCs \pm SEM: prior to 10 eIPSCs = 0.54 ± 0.12 sIPSCs/bin, prior to 25 eIPSCs = 0.48 ± 0.10 sIPSCs/bin, prior to 50 eIPSCs = 0.74 ± 0.10 sIPSCs/bin, $p > 0.05$).

The rate of delayed release was not only dependent on the stimulus duration, but also on the stimulation frequency (**Figure 5C,F** summary data for 6 cells). **Figure 5F**, shows that presynaptic activity determines the quantity and duration of asynchronous release (A or τ , 95% CI [lower, upper]: $A_{100Hz} = 12.4$ [10.8, 13.9] events, $A_{333Hz} = 28.3$ [26.0, 30.5] events, $p < 0.05$; $\tau_{100Hz} = 58.6$ [48.3, 74.7] ms, $\tau_{333Hz} = 78.5$ [69.3, 90.7] ms, $p < 0.05$, $n = 6$, fit comparison 100 Hz vs. 333 Hz $p < 0.001$, F -test).

The putative cause for the delayed asynchronous transmitter release is the accumulation of presynaptic calcium during high frequency IPSC trains. This can be experimentally enhanced by replacing the extracellular calcium with strontium, or alternatively, the effect can be reduced by applying a cell permeable calcium chelator that accelerates the decay of presynaptic calcium transients (Goda and Stevens, 1994; Atluri and Regehr, 1996, 1998; Lu and Trussell, 2000; Xu-Friedman and Regehr, 2000; Hefft and Jonas, 2005; Best and Regehr, 2009; Tang and Lu, 2012). To test whether the delayed asynchronous events can prolong the IPSCs decay times, their incidence was increased by replacing 2 mM extracellular calcium by 8 mM strontium (**Figures 6A–C**). In addition to a higher frequency of asynchronous events (A) shortly after the 100 Hz stimulation (10 eIPSCs), strontium also caused a prolongation of the time course (τ) of the last IPSC (**Figures 6B,C**; $n = 6$, mono-exponential fit comparison: $p < 0.001$, F -Test; A or τ 95% CI [lower, upper]: $A_{Ca^{2+}} = 6.8$ [5.7, 7.9] events, $A_{Sr^{2+}} = 21.2$ [19.4, 23.0] events; $\tau_{Ca^{2+}} = 13.5$ [9.4, 23.9] ms, $\tau_{Sr^{2+}} = 47.2$ [40.9, 55.8] ms, Ca^{2+} vs. Sr^{2+} $p < 0.05$). Consistent with the observation that asynchronous release strongly depends on synaptic activity (**Figure 5**), 8 mM strontium was more potent in prolonging the IPSC τ_{wd} following higher stimulation rate and longer stimulation (**Figure 6C**; Ca^{2+} vs. Sr^{2+} 100 Hz 10th $p < 0.05$; 333 Hz 50th $p < 0.01$, $n = 6$, RM ANOVA). Notably, single IPSC decays were not affected by the Ca^{2+} replacement ($p = 0.8$). These results suggest that the slow decay of IPSCs is indeed shaped by the asynchronous release which in turn is determined by the rate of presynaptic activity.

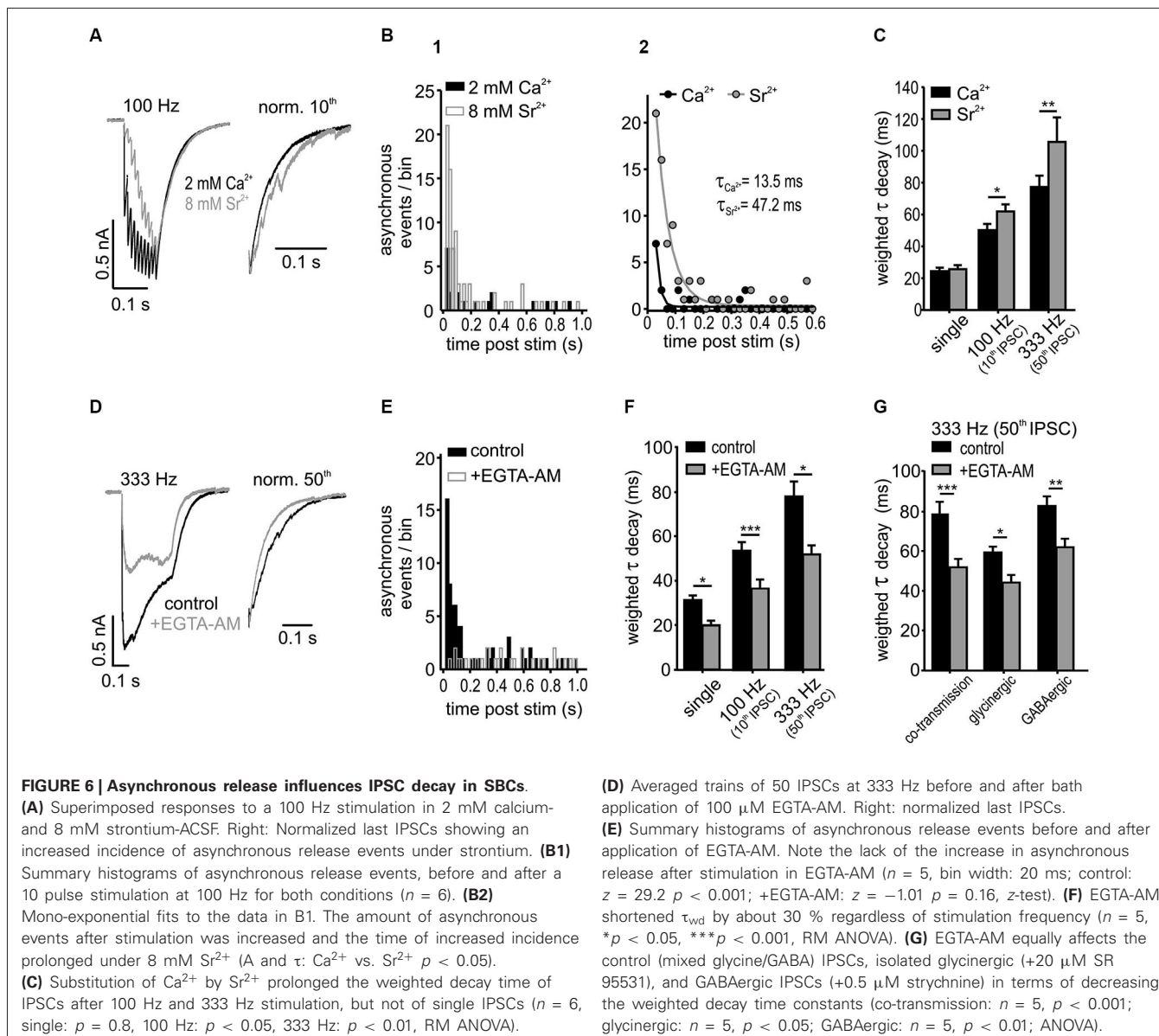
To further address this issue, the contribution of the delayed vesicle release to IPSC decay times was determined through reduction of presynaptic calcium with the calcium chelator EGTA-AM (100 μ M) (**Figures 6D–G**). The IPSC amplitudes strongly decreased under EGTA-AM by $55 \pm 8\%$ for single IPSC, $71 \pm 4\%$ for the 10th IPSC at 100 Hz and $55 \pm 10\%$ for 50th IPSC at 333 Hz, presumably due to a reduction in the peak Ca^{2+} concentration in the presynaptic terminal (Atluri and Regehr, 1996). The significant increase of asynchronous events observed in control condition after 333 Hz stimulation (50 IPSCs) vanished completely under EGTA-AM (**Figure 6E**; change of asynchronous events after stimulation compared to baseline level before stimulation: control $z = 29.2$, $p < 0.001$; +EGTA-AM $z = -1.01$, $p = 0.16$, z -test). Moreover, the weighted decay time constant was shortened by $30 \pm 3\%$ regardless of stimulus condition (**Figure 6F**; EGTA-AM effect vs. frequency $p = 0.9$, $n = 5$, RM ANOVA) and transmitter type (glycine, GABA or both) (**Figure 6G**; EGTA-AM effect vs. transmission type $p = 0.59$, $n = 5$ for each condition, ANOVA). Together, these data suggest that both glycine and GABA contribute to the delayed release and thereby shape the inhibitory current profile in an activity-dependent manner.

DISCUSSION

The mixed glycine-GABA transmission observed in SBCs is for the most part dominated by glycine but it still exhibits slow synaptic decays resulting in a long lasting, tonic-like inhibition. While glycine primarily contributes to the IPSC amplitudes, GABA enhances and prolongs the total inhibitory conductance, especially at higher firing rates (Nerlich et al., 2014). Here we demonstrate that the resulting IPSC decay strongly depends on both the synaptic activity and the number of recruited inhibitory fibers, each increasing the amount of transmitters released. The slow glycine and GABA clearance permits a longer availability of the transmitters in the synaptic cleft, thereby enabling transmitter rebinding and glycine spillover. Moreover, the IPSC kinetics is dynamically shaped by the delayed release of glycine and GABA. In addition to the shift towards slower GABAergic transmission at higher input rates (Nerlich et al., 2014), these activity-dependent mechanisms jointly determine the remarkably slow inhibition in SBCs.

TRANSMITTER REBINDING AND SPILLOVER CONTRIBUTE TO THE IPSC DECAY

The SBCs of the cochlear nucleus are the first synaptic center where primary auditory input from the cochlea is integrated with a higher-order, acoustically-evoked inhibition to preserve or improve temporal precision on the sub-millisecond scale (Gai and Carney, 2008; Dehmel et al., 2010; Kuenzel et al., 2011). Such synaptic inhibition is likely to contribute to the temporal synchronization of AP discharges to a particular phase of a low frequency tone burst (Joris et al., 1994; Paolini et al., 2001; Dehmel et al., 2010). Saying this, it should not be disregarded that also other previously discussed mechanisms (Nerlich et al., 2014), such as coincidence of presynaptic inputs also add to the synchronicity of postsynaptic SBC discharges (Kuhlmann et al., 2002; Xu-Friedman and Regehr, 2005). With



respect to the inhibitory effects, it was shown that an activity-dependent regulation of inhibitory strength mediated through a slow glycine-GABA transmission adjusts the fidelity at the endbulb of Held synapse towards fast rising and large EPSPs (Kuenzel et al., 2011; Xie and Manis, 2013; Nerlich et al., 2014). The present data further demonstrate that the inhibitory strength crucially depends on the presynaptic firing rate, which is of particular physiological importance given the weak inhibition at lower sound intensities, i.e., low firing rates (Kuenzel et al., 2011). Following strong inhibitory stimulation, slow glycine and GABA clearance from the synaptic cleft appears to enable ongoing rebinding of transmitters and intersynaptic pooling of glycine. A similar mechanism was previously shown to mediate prolonged inhibition of granule cells in the rat DCN (Balakrishnan et al., 2009) and of the nucleus laminaris neurons in the chick auditory brainstem (Tang and Lu,

2012). Several lines of evidence suggest that both the GlyT2 and the GABA transporters GAT1/3 contribute to the kinetics of activity-dependent inhibition at SBCs. Particularly, the slow decay phase (τ_{slow}) was affected by increasing stimulus frequencies, suggesting longer availability of transmitters. Similar τ_{slow} prolongation was also observed in the presence of glycine and GABA transporter antagonists. As the respective slowly decaying current is most likely due to slow transmitter clearance (Otis et al., 1996; Williams et al., 1998), our data are consistent with transporter saturation during higher neuronal activity. In line with this, the vesicular inhibitory amino acid transporter (VGAT), which depends on the supply of cytosolic transmitter to enable synaptic corelease of glycine and GABA (Wojcik et al., 2006), is apparently not the rate limiting factor for efficient refilling of inhibitory vesicles (Apostolides and Trussell, 2013).

At mixed glycine-GABA synapses, several factors determine the characteristics of the postsynaptic response: (i) the glycine/GABA ratio in synaptic vesicles which is not only determined by the higher VGAT affinity for glycine than for GABA (McIntire et al., 1997; Bedet et al., 2000); but also crucially depends on the availability of glycine through GlyT2 activity (Rousseau et al., 2008); and (ii) the postsynaptic receptor expression levels, clustering, and localizations (Todd et al., 1996; Dugué et al., 2005). In our recent study, we described a relative increase of the GABAergic component from 5 to 12% of the mixed IPSC amplitude during ongoing synaptic activity (Nerlich et al., 2014). When glycine and GABA were puff-applied (equimolar concentrations of 500 μM), the current amplitude ratio was $\sim 3:2$ (1.7:1.2 nA), indicating that GABA_AR availability is probably not the rate limiting factor for restricted GABAergic contribution to the IPSC. Presently, we found no evidence for GABA spillover to distant receptors that could account for the activity-dependent increase in the GABAergic proportion. Thus, the slow glycine clearance by GlyT2 and its low intracellular availability may possibly explain the progressively higher GABAergic signaling at *in vivo*-like firing rates.

Compared to the events elicited in 1.2 mM $[\text{Ca}^{2+}]_o$, IPSCs measured under the standard 2 mM $[\text{Ca}^{2+}]_o$ condition were found to be slower after shorter stimulus trains or at lower input rates, possibly indicating a contribution of multivesicular release. However, longer or high frequency stimulation (50 pulses at 100 Hz, 10 or 50 pulses at 333 Hz) evoked IPSC of comparable amplitudes towards the end of the train and the similar decay kinetics of the last event. This suggests that prolonged neuronal activity at physiological-like rates leads to a steady state transmitter level in the cleft, independent of the initial release probability. The data also argue against the prominent receptor desensitization, because its effect would render IPSCs faster with increasing transmitter concentrations at higher rates (Jones and Westbrook, 1996), which was not observed in our experiments.

Glycine receptor saturation and spillover onto nearby or distant receptors probably shapes the IPSC kinetics at physiologically relevant firing rates. Due to the lack of effect of the low-affinity GABA_A antagonist, we conclude that the respective receptors are probably tightly coupled to the release sites and unlikely to saturate. In line with this notion, is the lack of GABA_A $\alpha 6$ and δ subunit expression on SBCs (Campos et al., 2001) which were shown to constitute the extrasynaptic receptors (Nusser et al., 1998; Kullmann et al., 2005). The slow IPSC kinetics measured at SBCs contrast with respective data for other inhibitory auditory synapses with decay time constants < 5 ms, in which GABA is either not engaged or plays a minor role in determining the response decay time (Awatramani et al., 2004; Magnusson et al., 2005; Chirila et al., 2007; Couchman et al., 2010). As the SBC IPSCs progressively resembled the kinetics of pharmacologically isolated GABAergic events at increasing input frequencies, the mechanisms engaged with GABA release are likely to regulate the duration of inhibition at physiologically relevant rates (Nerlich et al., 2014). One possible contributing mechanism, though not a focus of the present study, is the kinetics of the GABA_A receptor

itself. The $\alpha 3$ subunit, linked to slow kinetics, deactivation- and desensitization rates (Verdoorn, 1994; Gingrich et al., 1995) is coexpressed with the subunits $\alpha 1$, $\alpha 5$, $\beta 3$ and $\gamma 2\text{L}$ in the rat AVCN (Campos et al., 2001). In olfactory bulb neurons of juvenile rats, the deactivation kinetics of GABA-evoked mIPSCs can span a τ_{wd} range of 3–30 ms through the expression of different compositions of the fast $\alpha 1$ and the slow $\alpha 3$ subunits in the receptor heteromers (Eyre et al., 2012). Therefore, it is conceivable that the specific composition of GABA_A subunits in SBCs partially contributes to an increase in τ_{wd} which ranged between 20–90 ms in an activity-dependent manner. Notably, even the isolated glycinergic spontaneous- and evoked-IPSCs exhibit slow synaptic decays (Xie and Manis, 2013, 2014; Nerlich et al., 2014). This may be surprising, given the general developmental down-regulation of the GlyR $\alpha 2$ subunit, associated with slower receptor kinetics (Veruki et al., 2007) in the cochlear nucleus and in the superior olivary complex (Sato et al., 1995; Friauf et al., 1997). However, the developmental replacement by the $\alpha 1$ subunit in the AVCN seems in the AVCN, as low levels of $\alpha 2$ mRNA were found up to the third postnatal week (Piechotta et al., 2001). Our data substantiate the hypothesis of a persistent $\alpha 2$ subunit expression throughout adulthood by showing that single pulse stimulation evokes IPSCs of similar τ_{wd} for pharmacologically isolated glycinergic, GABAergic, and mixed glycine-GABA events (Nerlich et al., 2014). Here, further corroboration is provided by showing comparable slow kinetics of the spontaneous IPSCs and IPSCs synaptically elicited in low release probability conditions. In both cases, the amount of released transmitters is presumed low, thus reducing the contribution of activity-dependent mechanisms. Although our results argue for a role of slow GlyR and GABA_AR, this still seems to be only an additional mechanism shaping the overall kinetic profile.

INHIBITORY KINETICS IS SHAPED BY THE ACTIVITY-INDUCED DELAYED RELEASE

Asynchronous (or delayed) transmitter release is another mechanism to generate a long-long lasting inhibition in the brain (Lu and Trussell, 2000; Hefft and Jonas, 2005; Tang and Lu, 2012). The ongoing synaptic activity can lead to Ca^{2+} accumulation in the presynaptic terminal, thereby causing the loss of coupling between the presynaptic AP and the release machinery (Chen and Regehr, 1999). Our data from the present and previous study (Nerlich et al., 2014) consistently show the activity-dependent change of release mode. The individual IPSCs were clearly segregated at 100 Hz, indicating synchronized quantal release, whereas the 333 Hz stimulation evoked a large plateau current caused by asynchronous release. Notably, the delayed asynchronous release events, mediated by both glycine and GABA, were observed at both frequencies during the decay phase of the last IPSC. The prominent effect of the slow calcium chelator EGTA-AM in our experiments, suggests a loose coupling between presynaptic Ca^{2+} channels and the Ca^{2+} sensor, possibly in a form of microdomains (Meinrenken et al., 2002; Eggermann et al., 2012; Vyleta and Jonas, 2014). The Ca^{2+} dependence of release machinery was, however, not in focus of the present study. Alongside transmitter rebinding and spillover, asynchronous

release is a major mechanism contributing to activity-dependent changes in inhibitory duration.

EFFICACY OF SLOW INHIBITION

Neurons in the auditory brainstem generate APs with an extraordinary temporal accuracy required for the computation of sound source location (for review see, Grothe et al., 2010). In the binaural nuclei of the superior olivary complex, the fast and mainly glycinergic inhibition may contribute by providing high precision phasic suppression of excitatory conductance (Awatramani et al., 2004; Magnusson et al., 2005; Chirila et al., 2007; Couchman et al., 2010; Roberts et al., 2013, 2014; Myoga et al., 2014). The monaural neurons in the mammalian cochlear nucleus, such as bushy cells of the AVCN and the granule cells of the DCN, on the other hand, utilize slow inhibition characterized by an activity-dependent conductance build-up (Balakrishnan et al., 2009; Xie and Manis, 2013). *In vivo*, the onset of acoustically evoked inhibition on SBCs is delayed compared to the excitation (Kuenzel et al., 2011; Nerlich et al., 2014) which cannot be solely explained by the polysynaptic inhibitory pathway causing a delay of just a few milliseconds (Smith and Rhode, 1989; Wickesberg and Oertel, 1990; Saint Marie et al., 1991; Ostapoff et al., 1997; Campagnola and Manis, 2014). Rather, the new data suggest that the slow time course of inhibition is predominantly determined by the receptor kinetics and transmitter clearance during short stimuli, whereas long duration or high frequency stimulation additionally engage spillover of glycine and asynchronous release of both glycine and GABA to prolong IPSCs. The contribution of these synaptic mechanisms can explain the slow onset of inhibition observed *in vivo*. With increasing sound intensity, the dynamic adjustment of inhibitory potency through synergistic glycine-GABA signaling (Nerlich et al., 2014) would ensure effective integration with strong and coincident excitatory inputs leading to non-monotonic rate-level functions and improved temporal precision of the SBC output (Kopp-Scheinflug et al., 2002; Dehmel et al., 2010; Kuenzel et al., 2011). Consistent with this hypothesis, a modeling study of SBC inhibition with fast IPSC kinetics as those measured in AVCN T-stellate cells impaired the temporal precision of spiking (Xie and Manis, 2013). Thus, the activity-dependence of slow inhibition seems to be a critical factor for precise temporal processing in SBCs.

ACKNOWLEDGMENTS

This work was supported by the DFG grants MI 954/2-1 (Ivan Milenkovic, Jana Nerlich), MI 954/1-1 (Ivan Milenkovic), RU 390/19-1 (Rudolf Rübsamen, Jana Nerlich), GRK 1097 (Jana Nerlich, C.K.), the NIH grant NIH/NIDCD R01-DC008989 (R. Michael Burger, Jana Nerlich), and a DAAD scholarship to Jana Nerlich. The authors thank Stefan N. Oline for helpful comments on an earlier version of the manuscript.

REFERENCES

- Apostolides, P. F., and Trussell, L. O. (2013). Rapid, activity-independent turnover of vesicular transmitter content at a mixed glycine/GABA synapse. *J. Neurosci.* 33, 4768–4781. doi: 10.1523/JNEUROSCI.5555-12.2013
- Apostolides, P. F., and Trussell, L. O. (2014). Chemical synaptic transmission onto superficial stellate cells of the mouse dorsal cochlear nucleus. *J. Neurophysiol.* 111, 1812–1822. doi: 10.1152/jn.00821.2013
- Atluri, P. P., and Regehr, W. G. (1996). Determinants of the time course of facilitation at the granule cell to Purkinje cell synapse. *J. Neurosci.* 16, 5661–5671.
- Atluri, P. P., and Regehr, W. G. (1998). Delayed release of neurotransmitter from cerebellar granule cells. *J. Neurosci.* 18, 8214–8227.
- Awatramani, G. B., Turecek, R., and Trussell, L. O. (2004). Inhibitory control at a synaptic relay. *J. Neurosci.* 24, 2643–2647. doi: 10.1523/jneurosci.5144-03.2004
- Awatramani, G. B., Turecek, R., and Trussell, L. O. (2005). Staggered development of GABAergic and glycinergic transmission in the MNTB. *J. Neurophysiol.* 93, 819–828. doi: 10.1152/jn.00798.2004
- Balakrishnan, V., Kuo, S. P., Roberts, P. D., and Trussell, L. O. (2009). Slow glycinergic transmission mediated by transmitter pooling. *Nat. Neurosci.* 12, 286–294. doi: 10.1038/nn.2265
- Beato, M. (2008). The time course of transmitter at glycinergic synapses onto motoneurons. *J. Neurosci.* 28, 7412–7425. doi: 10.1523/JNEUROSCI.0581-08.2008
- Bedet, C., Isambert, M. F., Henry, J. P., and Gasnier, B. (2000). Constitutive phosphorylation of the vesicular inhibitory amino acid transporter in rat central nervous system. *J. Neurochem.* 75, 1654–1663. doi: 10.1046/j.1471-4159.2000.0751654.x
- Best, A. R., and Regehr, W. G. (2009). Inhibitory regulation of electrically coupled neurons in the inferior olive is mediated by asynchronous release of GABA. *Neuron* 62, 555–565. doi: 10.1016/j.neuron.2009.04.018
- Borst, J. G. (2010). The low synaptic release probability in vivo. *Trends Neurosci.* 33, 259–266. doi: 10.1016/j.tins.2010.03.003
- Bradaia, A., Schlichter, R., and Trouslard, J. (2004). Role of glial and neuronal glycine transporters in the control of glycinergic and glutamatergic synaptic transmission in lamina X of the rat spinal cord. *J. Physiol.* 559(Pt. 1), 169–186. doi: 10.1113/jphysiol.2004.068858
- Campagnola, L., and Manis, P. B. (2014). A map of functional synaptic connectivity in the mouse anteroventral cochlear nucleus. *J. Neurosci.* 34, 2214–2230. doi: 10.1523/JNEUROSCI.4669-13.2014
- Campos, M. L., de Cabo, C., Wisden, W., Juiz, J. M., and Merlo, D. (2001). Expression of GABA(A) receptor subunits in rat brainstem auditory pathways: cochlear nuclei, superior olivary complex and nucleus of the lateral lemniscus. *Neuroscience* 102, 625–638. doi: 10.1016/s0306-4522(00)00525-x
- Capogna, M., and Pearce, R. A. (2011). GABA A, slow: causes and consequences. *Trends Neurosci.* 34, 101–112. doi: 10.1016/j.tins.2010.10.005
- Chanda, S., and Xu-Friedman, M. A. (2010). A low-affinity antagonist reveals saturation and desensitization in mature synapses in the auditory brain stem. *J. Neurophysiol.* 103, 1915–1926. doi: 10.1152/jn.00751.2009
- Chen, S., and Diamond, J. S. (2002). Synaptically released glutamate activates extrasynaptic NMDA receptors on cells in the ganglion cell layer of rat retina. *J. Neurosci.* 22, 2165–2173.
- Chen, C., and Regehr, W. G. (1999). Contributions of residual calcium to fast synaptic transmission. *J. Neurosci.* 19, 6257–6266.
- Chéry, N., and de Koninck, Y. (1999). Junctional versus extrajunctional glycine and GABA(A) receptor-mediated IPSCs in identified lamina I neurons of the adult rat spinal cord. *J. Neurosci.* 19, 7342–7355.
- Chirila, F. V., Rowland, K. C., Thompson, J. M., and Spirou, G. A. (2007). Development of gerbil medial superior olive: integration of temporally delayed excitation and inhibition at physiological temperature. *J. Physiol.* 584(Pt. 1), 167–190. doi: 10.1113/jphysiol.2007.137976
- Coleman, W. L., Fischl, M. J., Weimann, S. R., and Burger, R. M. (2011). GABAergic and glycinergic inhibition modulate monaural auditory response properties in the avian superior olivary nucleus. *J. Neurophysiol.* 105, 2405–2420. doi: 10.1152/jn.01088.2010
- Couchman, K., Grothe, B., and Felmy, F. (2010). Medial superior olivary neurons receive surprisingly few excitatory and inhibitory inputs with balanced strength and short-term dynamics. *J. Neurosci.* 30, 17111–17121. doi: 10.1523/JNEUROSCI.1760-10.2010
- Dehmel, S., Kopp-Scheinflug, C., Weick, M., Dörrscheidt, G. J., and Rübsamen, R. (2010). Transmission of phase-coupling accuracy from the auditory nerve to spherical bushy cells in the Mongolian gerbil. *Hear. Res.* 268, 234–249. doi: 10.1016/j.heares.2010.06.005
- Diamond, J. S. (2001). Neuronal glutamate transporters limit activation of NMDA receptors by neurotransmitter spillover on CA1 pyramidal cells. *J. Neurosci.* 21, 8328–8338.

- Dugué, G. P., Dumoulin, A., Triller, A., and Dieudonné, S. (2005). Target-dependent use of co-released inhibitory transmitters at central synapses. *J. Neurosci.* 25, 6490–6498. doi: 10.1523/jneurosci.1500-05.2005
- Dumoulin, A., Triller, A., and Dieudonné, S. (2001). IPSC kinetics at identified GABAergic and mixed GABAergic and glycinergic synapses onto cerebellar Golgi cells. *J. Neurosci.* 21, 6045–6057.
- Eggermann, E., Bucurenciu, I., Goswami, S. P., and Jonas, P. (2012). Nanodomain coupling between Ca²⁺ channels and sensors of exocytosis at fast mammalian synapses. *Nat. Rev. Neurosci.* 13, 7–21. doi: 10.1038/nrn3125
- Eyre, M. D., Renzi, M., Farrant, M., and Nusser, Z. (2012). Setting the time course of inhibitory synaptic currents by mixing multiple GABA(A) receptor α subunit isoforms. *J. Neurosci.* 32, 5853–5867. doi: 10.1523/JNEUROSCI.6495-11.2012
- Farrant, M., and Nusser, Z. (2005). Variations on an inhibitory theme: phasic and tonic activation of GABA(A) receptors. *Nat. Rev. Neurosci.* 6, 215–229. doi: 10.1038/nrn1625
- Fischl, M. J., Weimann, S. R., Kearse, M. G., and Burger, R. M. (2014). Slowly emerging glycinergic transmission enhances inhibition in the sound localization pathway of the avian auditory system. *J. Neurophysiol.* 111, 565–572. doi: 10.1152/jn.00640.2013
- Friauf, E., Hammerschmidt, B., and Kirsch, J. (1997). Development of adult-type inhibitory glycine receptors in the central auditory system of rats. *J. Comp. Neurol.* 385, 117–134. doi: 10.1002/(sici)1096-9861(19970818)385:1<117::aid-cne7>3.0.co;2-5
- Gai, Y., and Carney, L. H. (2008). Influence of inhibitory inputs on rate and timing of responses in the anteroventral cochlear nucleus. *J. Neurophysiol.* 99, 1077–1095. doi: 10.1152/jn.00708.2007
- Gingrich, K. J., Roberts, W. A., and Kass, R. S. (1995). Dependence of the GABAA receptor gating kinetics on the alpha-subunit isoform: implications for structure-function relations and synaptic transmission. *J. Physiol.* 489(Pt. 2), 529–543.
- Goda, Y., and Stevens, C. F. (1994). Two components of transmitter release at a central synapse. *Proc. Natl. Acad. Sci. U S A* 91, 12942–12946. doi: 10.1073/pnas.91.26.12942
- González-Forero, D., and Alvarez, F. J. (2005). Differential postnatal maturation of GABAA, glycine receptor and mixed synaptic currents in Renshaw cells and ventral spinal interneurons. *J. Neurosci.* 25, 2010–2023. doi: 10.1523/jneurosci.2383-04.2005
- Grothe, B., Pecka, M., and McAlpine, D. (2010). Mechanisms of sound localization in mammals. *Physiol. Rev.* 90, 983–1012. doi: 10.1152/physrev.00026.2009
- Hefft, S., and Jonas, P. (2005). Asynchronous GABA release generates long-lasting inhibition at a hippocampal interneuron-principal neuron synapse. *Nat. Neurosci.* 8, 1319–1328. doi: 10.1038/nn1542
- Husson, Z., Rousseau, C. V., Broll, I., Zeilhofer, H. U., and Dieudonné, S. (2014). Differential GABAergic and glycinergic inputs of inhibitory interneurons and purkinje cells to principal cells of the cerebellar nuclei. *J. Neurosci.* 34, 9418–9431. doi: 10.1523/JNEUROSCI.0401-14.2014
- Isaacson, J. S., and Walmsley, B. (1996). Amplitude and time course of spontaneous and evoked excitatory postsynaptic currents in bushy cells of the anteroventral cochlear nucleus. *J. Neurophysiol.* 76, 1566–1571.
- Jonas, P., Bischofberger, J., and Sandkühler, J. (1998). Corelease of two fast neurotransmitters at a central synapse. *Science* 281, 419–424. doi: 10.1126/science.281.5375.419
- Jones, M. V., and Westbrook, G. L. (1996). The impact of receptor desensitization on fast synaptic transmission. *Trends Neurosci.* 19, 96–101. doi: 10.1016/s0166-2236(96)80037-3
- Joris, P. X., Carney, L. H., Smith, P. H., and Yin, T. C. (1994). Enhancement of neural synchronization in the anteroventral cochlear nucleus. I. Responses to tones at the characteristic frequency. *J. Neurophysiol.* 71, 1022–1036.
- Keller, A. F., Coull, J. A., Chery, N., Poisbeau, P., and De Koninck, Y. (2001). Region-specific developmental specialization of GABA-glycine cosynapses in laminae I–II of the rat spinal dorsal horn. *J. Neurosci.* 21, 7871–7880.
- Keros, S., and Häblitz, J. J. (2005). Subtype-specific GABA transporter antagonists synergistically modulate phasic and tonic GABAA conductances in rat neocortex. *J. Neurophysiol.* 94, 2073–2085. doi: 10.1152/jn.00520.2005
- Kopp-Scheinpflug, C., Dehmel, S., Dörrscheidt, G. J., and Rübsamen, R. (2002). Interaction of excitation and inhibition in anteroventral cochlear nucleus neurons that receive large endbulb synaptic endings. *J. Neurosci.* 22, 11004–11018.
- Kramer, F., Griesemer, D., Bakker, D., Brill, S., Franke, J., Frotscher, E., et al. (2014). Inhibitory glycinergic neurotransmission in the mammalian auditory brainstem upon prolonged stimulation: short-term plasticity and synaptic reliability. *Front. Neural Circuits* 8:14. doi: 10.3389/fncir.2014.00014
- Kuenzel, T., Borst, J. G., and van der Heijden, M. (2011). Factors controlling the input-output relationship of spherical bushy cells in the gerbil cochlear nucleus. *J. Neurosci.* 31, 4260–4273. doi: 10.1523/JNEUROSCI.5433-10.2011
- Kuhlmann, L., Burkitt, A. N., Paolini, A., and Clark, G. M. (2002). Summation of spatiotemporal input patterns in leaky integrate-and-fire neurons: application to neurons in the cochlear nucleus receiving converging auditory nerve fiber input. *J. Comput. Neurosci.* 12, 55–73. doi: 10.1023/A:1014994113776
- Kullmann, D. M., Ruiz, A., Rusakov, D. M., Scott, R., Semyanov, A., and Walker, M. C. (2005). Presynaptic, extrasynaptic and axonal GABAA receptors in the CNS: where and why? *Prog. Biophys. Mol. Biol.* 87, 33–46. doi: 10.1016/j.pbiomolbio.2004.06.003
- Kuo, S. P., Bradley, L. A., and Trussell, L. O. (2009). Heterogeneous kinetics and pharmacology of synaptic inhibition in the chick auditory brainstem. *J. Neurosci.* 29, 9625–9634. doi: 10.1523/JNEUROSCI.0103-09.2009
- Lu, T., Rubio, M. E., and Trussell, L. O. (2008). Glycinergic transmission shaped by the corelease of GABA in a mammalian auditory synapse. *Neuron* 57, 524–535. doi: 10.1016/j.neuron.2007.12.010
- Lu, T., and Trussell, L. O. (2000). Inhibitory transmission mediated by asynchronous transmitter release. *Neuron* 26, 683–694. doi: 10.1016/s0896-6273(00)81204-0
- Magnusson, A. K., Kapfer, C., Grothe, B., and Koch, U. (2005). Maturation of glycinergic inhibition in the gerbil medial superior olive after hearing onset. *J. Physiol.* 568(Pt. 2), 497–512. doi: 10.1113/jphysiol.2005.094763
- McIntire, S. L., Reimer, R. J., Schuske, K., Edwards, R. H., and Jorgensen, E. M. (1997). Identification and characterization of the vesicular GABA transporter. *Nature* 389, 870–876.
- Meinrenken, C. J., Borst, J. G., and Sakmann, B. (2002). Calcium secretion coupling at calyx of held governed by nonuniform channel-vesicle topography. *J. Neurosci.* 22, 1648–1667.
- Monsivais, P., Yang, L., and Rubel, E. W. (2000). GABAergic inhibition in nucleus magnocellularis: implications for phase locking in the avian auditory brainstem. *J. Neurosci.* 20, 2954–2963.
- Myoga, M. H., Lehnert, S., Leibold, C., Felmy, F., and Grothe, B. (2014). Glycinergic inhibition tunes coincidence detection in the auditory brainstem. *Nat. Commun.* 5:3790. doi: 10.1038/ncomms4790
- Nerlich, J., Kuenzel, T., Keine, C., Korenic, A., Rübsamen, R., and Milenkovic, I. (2014). Dynamic fidelity control to the central auditory system: synergistic glycine/GABAergic inhibition in the cochlear nucleus. *J. Neurosci.* 34, 11604–11620. doi: 10.1523/jneurosci.0719-14.2014
- Nicol, M. J., and Walmsley, B. (2002). Ultrastructural basis of synaptic transmission between endbulbs of Held and bushy cells in the rat cochlear nucleus. *J. Physiol.* 539(Pt. 3), 713–723. doi: 10.1113/jphysiol.2001.012972
- Nusser, Z., Sieghart, W., and Somogyi, P. (1998). Segregation of different GABAA receptors to synaptic and extrasynaptic membranes of cerebellar granule cells. *J. Neurosci.* 18, 1693–1703.
- O'Brien, J. A., and Berger, A. J. (1999). Cotransmission of GABA and glycine to brain stem motoneurons. *J. Neurophysiol.* 82, 1638–1641.
- Ostapoff, E. M., Benson, C. G., and Saint Marie, R. L. (1997). GABA- and glycine-immunoreactive projections from the superior olivary complex to the cochlear nucleus in guinea pig. *J. Comp. Neurol.* 381, 500–512. doi: 10.1002/(sici)1096-9861(19970519)381:4<500::aid-cne9>3.0.co;2-6
- Otis, T. S., Wu, Y. C., and Trussell, L. O. (1996). Delayed clearance of transmitter and the role of glutamate transporters at synapses with multiple release sites. *J. Neurosci.* 16, 1634–1644.
- Overstreet, L. S., and Westbrook, G. L. (2003). Synapse density regulates independence at unitary inhibitory synapses. *J. Neurosci.* 23, 2618–2626.
- Paolini, A. G., FitzGerald, J. V., Burkitt, A. N., and Clark, G. M. (2001). Temporal processing from the auditory nerve to the medial nucleus of the trapezoid body in the rat. *Hear. Res.* 159, 101–116. doi: 10.1016/s0378-5955(01)00327-6
- Piechotta, K., Weth, F., Harvey, R. J., and Friauf, E. (2001). Localization of rat glycine receptor alpha1 and alpha2 subunit transcripts in the developing auditory brainstem. *J. Comp. Neurol.* 438, 336–352. doi: 10.1002/cne.1319.abs
- Protti, D. A., Gerschenfeld, H. M., and Llano, I. (1997). GABAergic and glycinergic IPSCs in ganglion cells of rat retinal slices. *J. Neurosci.* 17, 6075–6085.

- Roberts, M. T., Seeman, S. C., and Golding, N. L. (2013). A mechanistic understanding of the role of feedforward inhibition in the mammalian sound localization circuitry. *Neuron* 78, 923–935. doi: 10.1016/j.neuron.2013.04.022
- Roberts, M. T., Seeman, S. C., and Golding, N. L. (2014). The relative contributions of MNTB and LNTB neurons to inhibition in the medial superior olive assessed through single and paired recordings. *Front. Neural Circuits* 8:49. doi: 10.3389/fncir.2014.00049
- Rousseau, F., Aubrey, K. R., and Supplisson, S. (2008). The glycine transporter GlyT2 controls the dynamics of synaptic vesicle refilling in inhibitory spinal cord neurons. *J. Neurosci.* 28, 9755–9768. doi: 10.1523/jneurosci.0509-08.2008
- Rousseau, C. V., Dugué, G. P., Dumoulin, A., Mugnaini, E., Dieudonné, S., and Diana, M. A. (2012). Mixed inhibitory synaptic balance correlates with glutamatergic synaptic phenotype in cerebellar unipolar brush cells. *J. Neurosci.* 32, 4632–4644. doi: 10.1523/jneurosci.5122-11.2012
- Russier, M., Kopysova, I. L., Ankril, N., Ferrand, N., and Debanne, D. (2002). GABA and glycine co-release optimizes functional inhibition in rat brainstem motoneurons in vitro. *J. Physiol.* 541(Pt. 1), 123–137. doi: 10.1113/jphysiol.2001.016063
- Ryugo, D. K., and Sento, S. (1991). Synaptic connections of the auditory nerve in cats: relationship between endbulbs of held and spherical bushy cells. *J. Comp. Neurol.* 305, 35–48. doi: 10.1002/cne.903050105
- Saint Marie, R. L., Benson, C. G., Ostapoff, E. M., and Morest, D. K. (1991). Glycine immunoreactive projections from the dorsal to the anteroventral cochlear nucleus. *Hear. Res.* 51, 11–28. doi: 10.1016/0378-5955(91)90003-r
- Sato, K., Kuriyama, H., and Altschuler, R. A. (1995). Expression of glycine receptor subunits in the cochlear nucleus and superior olivary complex using non-radioactive in-situ hybridization. *Hear. Res.* 91, 7–18. doi: 10.1016/0378-5955(95)00156-5
- Seddik, R., Schlichter, R., and Trouslard, J. (2007). Corelease of GABA/glycine in lamina-X of the spinal cord of neonatal rats. *Neuroreport* 18, 1025–1029. doi: 10.1097/wnr.0b013e3281667c0c
- Smith, P. H., and Rhode, W. S. (1989). Structural and functional properties distinguish two types of multipolar cells in the ventral cochlear nucleus. *J. Comp. Neurol.* 282, 595–616. doi: 10.1002/cne.902820410
- Song, I., Volynski, K., Brenner, T., Ushkaryov, Y., Walker, M., and Semyanov, A. (2013). Different transporter systems regulate extracellular GABA from vesicular and non-vesicular sources. *Front. Cell. Neurosci.* 7:23. doi: 10.3389/fncel.2013.00023
- Szabadics, J., Tamás, G., and Soltesz, I. (2007). Different transmitter transients underlie presynaptic cell type specificity of GABA_A, slow and GABA_A, fast. *Proc. Natl. Acad. Sci. U S A* 104, 14831–14836. doi: 10.1073/pnas.0707204104
- Takahashi, T., Momiyama, A., Hirai, K., Hishinuma, E., and Akagi, H. (1992). Functional correlation of fetal and adult forms of glycine receptors with developmental changes in inhibitory synaptic receptor channels. *Neuron* 9, 1155–1161. doi: 10.1016/0896-6273(92)90073-m
- Tang, Z.-Q., Dinh, E. H., Shi, W., and Lu, Y. (2011). Ambient GABA-activated tonic inhibition sharpens auditory coincidence detection via a depolarizing shunting mechanism. *J. Neurosci.* 31, 6121–6131. doi: 10.1523/jneurosci.4733-10.2011
- Tang, Z.-Q., and Lu, Y. (2012). Two GABA responses with distinct kinetics in a sound localization circuit. *J. Physiol.* 590(Pt. 16), 3787–3805. doi: 10.1113/jphysiol.2012.230136
- Thomas, C. G., Tian, H., and Diamond, J. S. (2011). The relative roles of diffusion and uptake in clearing synaptically released glutamate change during early postnatal development. *J. Neurosci.* 31, 4743–4754. doi: 10.1523/jneurosci.5953-10.2011
- Todd, A. J., Watt, C., Spike, R. C., and Sieghart, W. (1996). Colocalization of GABA, glycine and their receptors at synapses in the rat spinal cord. *J. Neurosci.* 16, 974–982.
- Verdoorn, T. A. (1994). Formation of heteromeric gamma-aminobutyric acid type A receptors containing two different alpha subunits. *Mol. Pharmacol.* 45, 475–480.
- Veruki, M. L., Gill, S. B., and Hartveit, E. (2007). Spontaneous IPSCs and glycine receptors with slow kinetics in wide-field amacrine cells in the mature rat retina. *J. Physiol.* 581(Pt. 1), 203–219. doi: 10.1113/jphysiol.2006.127316
- Vyleta, N. P., and Jonas, P. (2014). Loose coupling between Ca²⁺ channels and release sensors at a plastic hippocampal synapse. *Science* 343, 665–670. doi: 10.1126/science.1244811
- Wang, P., and Slaughter, M. M. (2005). Effects of GABA receptor antagonists on retinal glycine receptors and on homomeric glycine receptor alpha subunits. *J. Neurophysiol.* 93, 3120–3126. doi: 10.1152/jn.01228.2004
- Wentzel, P. R., De Zeeuw, C. I., Holstege, J. C., and Gerrits, N. M. (1993). Colocalization of GABA and glycine in the rabbit oculomotor nucleus. *Neurosci. Lett.* 164, 25–29. doi: 10.1016/0304-3940(93)90848-f
- Wickesberg, R. E., and Oertel, D. (1990). Delayed, frequency-specific inhibition in the cochlear nuclei of mice: a mechanism for monaural echo suppression. *J. Neurosci.* 10, 1762–1768.
- Williams, S. R., Buhl, E. H., and Mody, I. (1998). The dynamics of synchronized neurotransmitter release determined from compound spontaneous IPSCs in rat dentate granule neurones in vitro. *J. Physiol.* 510(Pt. 2), 477–497. doi: 10.1111/j.1469-7793.1998.477bk.x
- Wojcik, S. M., Katsurabayashi, S., Guillemain, I., Friauf, E., Rosenmund, C., Brose, N., et al. (2006). A shared vesicular carrier allows synaptic corelease of GABA and glycine. *Neuron* 50, 575–587. doi: 10.1016/j.neuron.2006.04.016
- Xie, R., and Manis, P. B. (2013). Target-specific IPSC kinetics promote temporal processing in auditory parallel pathways. *J. Neurosci.* 33, 1598–1614. doi: 10.1523/jneurosci.2541-12.2013
- Xie, R., and Manis, P. B. (2014). GABAergic and glycinergic inhibitory synaptic transmission in the ventral cochlear nucleus studied in VGAT channelrhodopsin-2 mice. *Front. Neural Circuits* 8:84. doi: 10.3389/fncir.2014.00084
- Xu-Friedman, M. A., and Regehr, W. G. (2000). Probing fundamental aspects of synaptic transmission with strontium. *J. Neurosci.* 20, 4414–4422.
- Xu-Friedman, M. A., and Regehr, W. G. (2005). Dynamic-clamp analysis of the effects of convergence on spike timing. II. Few synaptic inputs. *J. Neurophysiol.* 94, 2526–2534. doi: 10.1152/jn.01308.2004

Conflict of Interest Statement: The authors declare that the research was conducted in the absence of any commercial or financial relationships that could be construed as a potential conflict of interest.

Received: 12 September 2014; accepted: 02 December 2014; published online: 23 December 2014.

Citation: Nerlich J, Keine C, Rübsamen R, Burger RM and Milenkovic I (2014) Activity-dependent modulation of inhibitory synaptic kinetics in the cochlear nucleus. *Front. Neural Circuits* 8:145. doi: 10.3389/fncir.2014.00145

This article was submitted to the journal *Frontiers in Neural Circuits*.

Copyright © 2014 Nerlich, Keine, Rübsamen, Burger and Milenkovic. This is an open-access article distributed under the terms of the Creative Commons Attribution License (CC BY). The use, distribution and reproduction in other forums is permitted, provided the original author(s) or licensor are credited and that the original publication in this journal is cited, in accordance with accepted academic practice. No use, distribution or reproduction is permitted which does not comply with these terms.